

CANNONBALL MODEL DIAGNOSIS OF THE SHORT GAMMA RAY BURST 170817A

SHLOMO DADO,¹ ARNON DAR,¹ AND A. DE RÚJULA²

¹*Physics Department, Technion, Haifa 32000, Israel*

²*Theory Division, CERN, Geneva, Switzerland; IFT, Universidad Autónoma, Madrid, Spain*

ABSTRACT

The rich and complex data obtained from multi-wavelength observations of SHB170817A, the short hard gamma ray burst (SHB) associated with GW170817 –the first neutron stars merger event detected in gravitational waves (GWs)– are analyzed in the framework of the cannonball model of SHBs. In this model a highly relativistic jet is launched by fall back matter on the nascent neutron star (or black hole) into a surrounding glory (light from the surrounding wind nebula of the binary neutron stars) which was present already before the merger. The SHB was produced by inverse Compton scattering of glory photons by the jet, which was viewed far off-axis. The fading glory, which produced the initial UVOIR afterglow, was powered by a neutron star remnant. It was overtaken by a late time X-ray, UVOIR and radio afterglow produced by synchrotron radiation from the decelerating jet in the interstellar medium of the host galaxy. If the radio afterglow of SHB170817A was indeed produced by the jet, it should display a superluminal motion relative to the SHB location, still detectable in VLA and VLBI radio observations.

Keywords: gamma-ray burst, jet, neutron star, stellar black hole

1. INTRODUCTION

Gamma ray bursts (GRBs) were discovered fifty years ago by the American spy satellites Vela (Klebesadel, Strong & Olson 1973). For decades their origin and production mechanism remained mysterious. Thirty years ago, Goodman, Dar and Nussinov (1987) suggested that GRBs may be produced in extragalactic neutron star mergers (NSMs) by an $e^+e^-\gamma$ fireball (Goodman 1986) formed by neutrino-antineutrino annihilation around the nascent compact object – a massive neutron star or a black hole. But shortly after the launch of the Compton Gamma-Ray Burst Observatory (CGRO), it became clear that such neutrino-annihilation fireballs are not powerful enough to produce observable GRBs at the very large cosmological distances indicated by the CGRO observations (Meegan et al. 1992).

Consequently, Meszaros and Rees (1992) suggested that the $e^+e^-\gamma$ fireball produced in compact mergers may be collimated into a conical fireball by funneling through surrounding matter. Shaviv and Dar (1995), however, argued that GRBs are produced by inverse Compton scattering (ICS) of the surrounding light (glory) by narrowly collimated jets of highly relativistic plasmoids (cannonballs, CBs) of ordinary matter, launched in mergers of compact stars due to the emission of gravitational waves (GWs), in phase transition of neutron stars to quark stars in compact binaries following mass accretion, or in stripped-envelope core-collapse supernova explosions (Dar et al. 1992). Li and Paczynski (1998), countered that all GRBs are produced by macronovae, i.e., are the thermal radiation emitted from fireballs formed by the radioactive decay of r-process elements synthesized from the tidally-disrupted neutron-star surface material in compact binaries undergoing a merger by GW emission.

It has also been observed long ago that GRBs may be roughly classified into two distinct species, long-duration soft gamma-ray bursts (GRBs) that usually last more than 2 seconds and short hard bursts (SHBs) typically lasting less than 2 seconds (Norris et al. 1984; Kouveliotou et al. 1993), and that a large fraction of GRBs are produced in broad line stripped envelope supernova (SN) explosions of type Ic akin to SN1998bw (see Galama et al. 1998 for the first observed GRB-SN association; Dado et al. 2002, Zeh et al. 2004 and references therein for early photometric evidence; Stanek et al. 2003 and Hjorth et al. 2003 for the first spectroscopic evidence, and Della Valle et al. 2016 for a recent review. See also Dado, Dar & De Rújula 2003 for the prediction of the discovery date and properties of the SN associated with GRB030329).

Based on indirect evidence, it was widely believed that SHBs were associated with NSMs (see, e.g., Fong and Berger 2013, Berger 2014). In particular, a faint infrared emission from SHB130603B was claimed to be the first observational evidence for a macronova produced by a NSM (e.g. Berger et al. 2013, Tanvir et al. 2013). The first indisputable NSM-SHB association, i.e., GW170817-SHB170817A, was observed only recently (von Kienlin et al. 2017, Abbott et al. 2017a,b,c, Goldstein et al. 2017). Two days before these ground breaking observations, Dado and Dar predicted (2017) that because of the relatively small horizon of Ligo-Virgo for detection of NSMs by gravitational waves, *only far off-axis SHBs or orphan afterglows, but not ordinary SHBs, will accompany Ligo-Virgo detections of NSMs.*

The underlying process in the cannonball (CB) model of GRBs and SHBs is the ejection of highly-relativistic narrowly-collimated jets of CBs in stripped-envelope SNeIc and NSMs, respectively (e.g., Dar & De Rújula 2004; Dado, Dar & De Rújula 2002, 2009a; Dado, Dar & De Rújula 2009b). The ejections of CBs may take place after the merger by accretion of fall back matter from mass ejections sometime before the end of the merger process. Such a delayed ejection may explain the ~ 1.74 s delay in the arrival of the electromagnetic radiation after the arrival of the gravitational waves (von Kienlin et al. 2017; Abbott et al. 2017a,b,c; Goldstein et al. 2017).

In the CB model, the gamma-ray generating mechanism is ICS of a glory light (light scattered or emitted by winds or earlier mass ejections). The natural candidate producing such a glory is a pulsar wind nebula (Weiler & Panagia 1978, for a review, see, e.g., Gaensler & Slane 2006). Such a pulsar wind nebula (PWN) absorbs the magnetic dipole radiation and relativistic wind, which are emitted from the pulsar and converts most of its spin-down energy to synchrotron radiation in the radio, optical and X-ray bands, with approximately a broken power-law spectrum or an exponentially cutoff power-law spectrum and peak energy flux around 1 eV (see, e.g., Macias-Perez et al. 2010; Tanaka & Takahara 2010 and references therein).

The observed duration of the SHB pulses in ordinary SHBs requires a glory of a typical size $\sim 10^{15}$ cm. Such a relatively small size PWN may be quite natural for very compact neutron stars (n^* s) binaries. Assuming that both neutron stars may be approximated as point masses, circular n^*n^* binary orbit decays at a rate $da/dt = -a/t_{GW}$, where a is the binary separation and the merger timescale due to the gravitational radiation is given in geometrized units ($G=c=1$) by $t_{GW} = (5/64)a^4/\mu M^2$. $M = M_1 + M_2$ is the total

mass and $\mu = M_1 M_2 / (M_1 + M_2)$ is the reduced mass of the n^*n^* binary. For canonical neutron stars, with $M_1 = M_2 = 1.4M_\odot$ and initial separation a , the merger time due to gravitational radiation is $t_m = \int (dt/da) da \approx 1.76 (a/2R_\odot)^4$ Gy. This suggests that n^*n^* binaries with a merger time much shorter than the Hubble time must be born in very compact binaries. Such compact binaries may be formed either in a single SN explosion of a massive star by fission of its fast rotating core during its rapid collapse, or in two separate SN explosions in massive star binaries where dynamical friction in a common envelope phase shrinks the binary separation (e.g., Bhattacharya & van den Heuvel 1991; Lorimer 2008 and references therein).

In this paper we show that ICS of photons emitted by a PWN surrounding merging neutron stars, by a highly relativistic jet of CBs launched in the NSM and viewed far off-axis, can explain the prompt emission in SHB170817A, provided that the typical size of the PWN around NSMs is $R \sim 10^{15}$ cm, the PWN luminosity peaks around 1 eV, and the typical bulk motion Lorentz factor of the CBs, which produce SHBs, is $\gamma \sim 10^3$ (Dado et al. 2009b). The PWN may have a disk-like shape, or a torus-like shape, or even a more complicated shape.

In our CB model analysis, the absence of an extended X-ray emission in SHB170817A (Troja et al. 2017a,b), following the prompt γ -ray emission, is explained by the merger site *not* being in a densely illuminated region (Levan et al. 2017), unlike globular clusters where probably a considerable fraction of SHBs occur (Dado et al. 2009b).

The observed early time UVOIR afterglow is explained by light emission from an expanding fireball formed and powered by the ejecta, winds, radiations and high energy particles emitted from the merging n^* s and the nascent n^* , before and after the merger, respectively.

The observed late-time radio (Hallinan et al. 2017, Mooley et al. 2018) to X-ray (Troja et al. 2017a,b) afterglow, is explained by synchrotron radiation from the far off-axis decelerating jet. If the radio afterglow is emitted by the jet, it should display a superluminal motion relative to the SHB's location (Dar & De Rújula 2000a, Dado, Dar & De Rújula 2016) hopefully still detectable by VLA and VLBI radio observations.

2. THE PROMPT EMISSION

In the CB model SHBs and GRBs share many properties, since they are produced by the same mechanism: ICS of ambient light by a narrow jet of CBs with large Lorentz factors $\gamma \gg 1$. Their most probable viewing angles relative to the approaching-jet direction are $\theta \approx 1/\gamma$

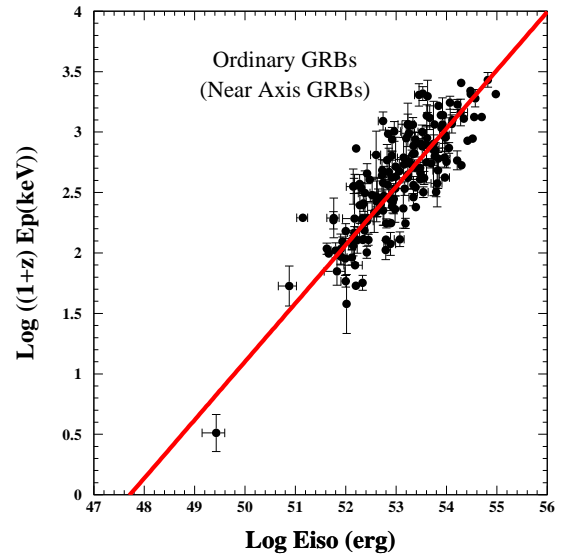


Figure 1. The $[E_p, E_{iso}]$ correlation for ordinary GRBs viewed near axis. The line is the CB model prediction of Eq.(1).

and the polarization of their radiation is predicted to be linear and large: $\Pi = 2\gamma^2 \theta^2 / (1 + \gamma^4 \theta^4) \approx 1$ (Shaviv & Dar 1995; Dar & De Rújula 2004 and references therein), while very near axis and far off-axis GRBs and SHBs should display a small polarization.

The CB model entails very simple correlations between the main observables of SHBs and GRBs (Dar & De Rújula 2000a). For a burst at redshift z and Doppler factor $\delta \simeq 2\gamma / (1 + \gamma^2 \theta^2)$, for instance, the peak energy of their time-integrated energy spectrum satisfies $(1+z)E_p \propto \gamma \delta$, while their isotropic-equivalent total gamma-ray energy is $E_{iso} \propto \gamma \delta^3$. Hence, ordinary GRBs and SHBs, mostly viewed from an angle $\theta \approx 1/\gamma$, obey

$$(1+z)E_p \propto [E_{iso}]^{1/2}, \quad (1)$$

while the far off-axis ($\theta^2 \gg 1/\gamma^2$) ones satisfy

$$(1+z)E_p \propto [E_{iso}]^{1/3}. \quad (2)$$

Updated results on the correlation of Eq.(1), later empirically discovered by Amati et al. (2002), are shown in Figure 1. They satisfy well the CB model predicted correlation for ordinary GRBs.

In Figure 2 we plot the observations for the correlation Eq.(2) for far off-axis GRBs (Dar & De Rújula 2000a), which is also well satisfied.

In Figure 3 we plot results for the entire population of SHBs with known z , E_p and E_{iso} , along with the predictions of Eqs.(1),(2). Ordinary (near axis) SHBs satisfy Eq.(1). The prediction of Eq.(2) for low luminosity (far

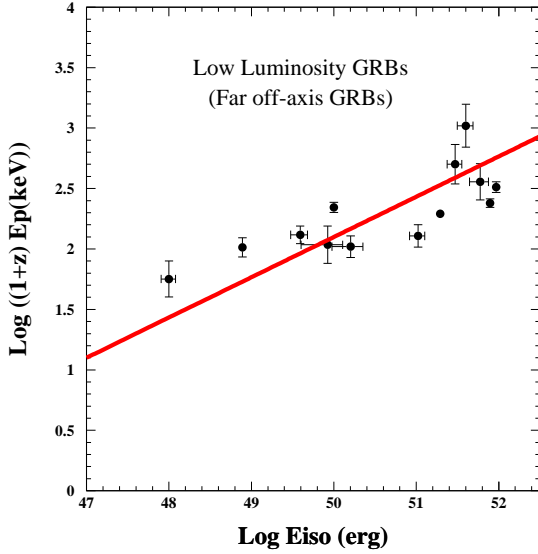


Figure 2. The $[E_p, E_{iso}]$ correlation of low luminosity (far off-axis) GRBs. The line is the CB model prediction of Eq.(2).

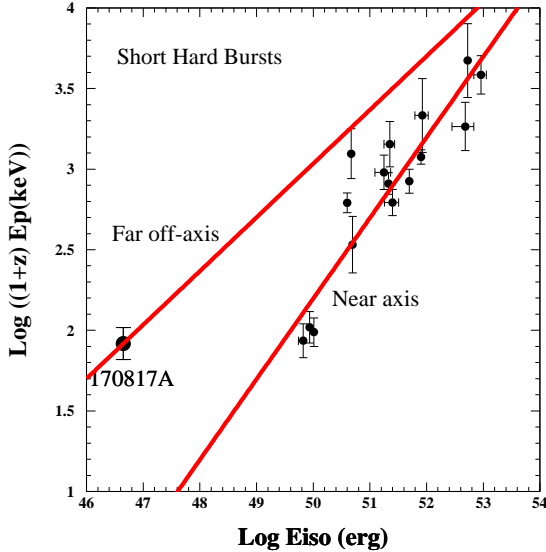


Figure 3. The $[E_p, E_{iso}]$ correlation for SHBs with known redshift. The lines are the CB model prediction of Eqs.(1),(2) for near and far off axis cases.

off-axis) SHBs cannot be tested because of the incompleteness of the current data (unknown E_p and/or z) on the few low luminosity SHBs.

Far off-axis viewing angles yield $\gamma \delta \approx 2/\theta^2$. Hence, ICS of a standard candle glory light with a peak photon energy $\epsilon_p \approx 1 \text{ eV}$, by a jet viewed from far off-axis yields an SHBs with $(1+z)E_p \approx 2 \text{ eV}/\theta^2$. Thus, the T_{90}

measured $E_p = 82 \pm 23 \text{ keV}$ of SHB170817A (von Kienlin et al. 2017) implies a viewing angle $\theta = \sqrt{2/82 \times 10^3} \approx 5 \times 10^{-3}$ (the value $E_p \approx 65 + 35/-14 \text{ keV}$, estimated by Pozanenko et al. (2018) from the same data yields $\theta \approx 5.5 \times 10^{-3}$). Such E_p is well above that expected from Eq.(1). But it is what is expected from Eq.(2), if the relatively small $E_{iso} \approx 5.4 \times 10^{46} \text{ erg}$ (Goldstein et al. 2017) is due to being viewed far off-axis. The same conclusion can also be drawn from its observed late-time X-ray afterglow (Troja et al. 2017a,b), which is simply impossible to fit in the CB model with $\gamma \theta \sim 1$, as we shall see in detail in Section 6. Such a viewing angle is similar to that of the first-detected far off-axis GRB 980425. In many respects, SHB170817A-NSM170817 is similar to GRB980425-SN1998bw, both of which were the first of their kind.

In the Thomson regime ($2\gamma\epsilon \ll m_e c^2$), the distribution of the incident photons after Compton scattering in the CB is nearly isotropic. In the observer frame this distribution becomes $dN_\gamma/d\Omega = N_\gamma \delta^2/4\pi$. The canonical $\gamma=1000$ of ordinary SHBs (e.g., Dado et al. 2009b) and the viewing angle $\theta=5 \text{ mrad}$ yield $\delta=80$. Consequently, in the CB model (Dar & De Rújula 2004), the measured $E_{iso} \approx 5.4 \times 10^{46} \text{ erg}$ (Goldstein et al. 2017) and $E_p = 82 \text{ keV}$ (von Kienlin et al. 2017) in SHB170817A, yield a total number of ICS photons $N_\gamma = E_{iso}/E_p \delta^2 \approx 6.4 \times 10^{49}$, and a total γ -ray energy $E_\gamma \approx \epsilon_p \gamma^2 N_\gamma \approx 1.0 \times 10^{44} \text{ erg}$.

Assuming that ejected CBs in NSMs are made of n^* surface material, i.e., mainly iron nuclei with roughly equal number of protons and neutrons (Chamel & Haensel 2008, and references therein), and that the kinetic energy of the CB electrons powers the prompt γ -ray emission by ICS of glory light, then, in the CB model, the estimated kinetic energy of the CB in SHB170817A was $E_k \approx 2 m_p E_\gamma/m_e \approx 3.7 \times 10^{47} \text{ erg}$, and its baryon number was $N_b \approx E_k/m_p c^2 \gamma \approx 2.5 \times 10^{47}$.

The peak time Δ of the prompt emission pulse is reached when the CB becomes transparent to photons, i.e., when the photon's mean diffusion time t_d out of the CB satisfies $R_{cb}^2/(c\lambda) = \Delta$. The photon's mean free path λ that is dominated by Thomson scattering on free electrons is given by $\lambda = 4\pi R_{cb}^3/(N_e \sigma_T)$ where $\sigma_T = 0.67 \times 10^{-24} \text{ cm}^2$ is Thomson cross section, and the electron number of the CB satisfies $N_e \approx N_b/2$. Thus, the peak time of the ICS pulse in SHB170817A formed by CB with $N_e \approx N_b/2 \approx 1.25 \times 10^{47}$, which is expanding with a speed of sound in a relativistic gas, $v = c/\sqrt{3}$, is expected to occur at $\Delta \approx 3\sqrt{3} N_e \sigma_T / 4\pi c^2 \delta = 0.69 \text{ s}$.

The mean photon density n_g of the glory in the volume V where from the SHB photons were scattered, satisfies $N_\gamma = n_g V \approx n_g \pi \gamma \delta^3 c^3 \Delta^3/9$. It yields $n_g \approx$

$4.0 \times 10^{10} \text{ cm}^{-3}$ for a peak time $\Delta \approx 0.69$ s of the prompt emission pulse of SHB170817A.

Note that while the CB model can predict the approximate pulse shape of single pulses (given their E_{iso} , E_p and R), it cannot predict the entire light curve of multi-pulse GRBs and SHBs, because neither the time sequence, nor the emission directions, nor the physical parameters of CBs are predictable. Moreover, a shotgun configuration of the emitted CBs, and/or a precession of the emission direction, as observed in pulsars and microquasars, combined with relativistic beaming, can make only a small fraction of the emitted CBs visible. That, and the very near distances of SHB170817A and GRB980425 can enhance the detection rate of such events by a large factor compared to that estimated from the assumption that only the CBs which produced the observed light curves were actually emitted.

For instance, long GRBs are detected by the Fermi GBM at a rate roughly 6 times larger than the detection rate of SHBs. The current horizon of Ligo-Virgo for detection of n*n* mergers is roughly 180 Mpc. During the past 12 years, 2 GRBs were detected with a redshift within this horizon (060218 and 111005A). If GRBs and SHBs have the same redshift distribution, then an event like SHB170817A should be detected by a Fermi GBM like detectors at a rate roughly once in 30 years, unless NSM170817 has launched many more CBs in a shotgun configuration or in succession along a precessing axis, out of which only 2 were detected by the Fermi GBM (von Kienlin et al. 2017; Goldstein et al. 2017).

3. PULSE SHAPE

In the absence of a detailed knowledge of the properties of the glory around n*n* mergers, and in view of the small statistics of the γ -ray data on SHB170817A (Goldstein et al. 2017), we perform only an approximate test of the CB model predictions for the temporal and spectral behaviors of its prompt γ -ray emission.

The observed pulse-shape produced by ICS of glory light with an exponentially cut off power law (CPL) spectrum, $dn_g/d\epsilon \propto \epsilon^{-\alpha} \exp(-\epsilon/\epsilon_p)$ at redshift z , by a CB is given approximately (see, e.g., Eq. (12) in Dado et al. 2009b) by

$$E \frac{d^2 N_\gamma}{dE dt} \propto \frac{t^2}{(t^2 + \Delta^2)^2} E^{1-\alpha} \exp(-E/E_p(t)) \quad (3)$$

where Δ is approximately the peak time of the pulse in the observer frame, which occurs when the CB becomes transparent to its internal radiation and $E_p \approx E_p(t = \Delta)$.

In Eq.(3), the early temporal rise like t^2 is produced by the increasing cross section, $\pi R_{CB}^2 \propto t^2$, of the fast expanding CB when it is still opaque to radiation (mainly

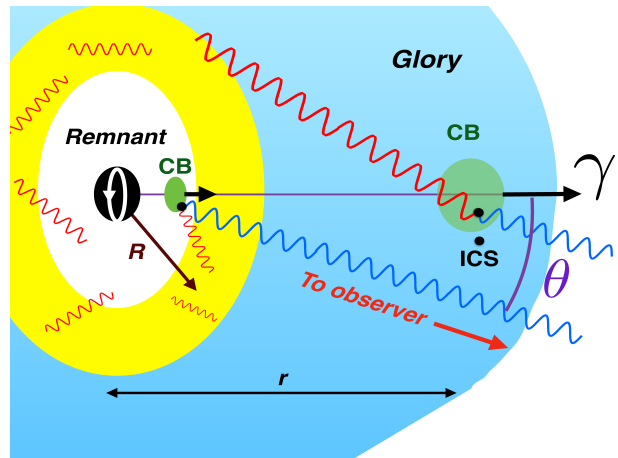


Figure 4. A CB as it crosses and exits the blue glory of a yellow toroidal PWN around NSM. The CB's electrons Compton up-scatter glory photons with incident angles which decrease with increasing distance from the CB launch point.

due to Compton scattering from its electrons when it is still very hot and completely ionized). When the CB becomes transparent to radiation due to its fast expansion, its cross section for ICS becomes $\sigma_T N_e$ where σ_T is the Thomson cross section, and N_e , the electron number of the CB, is roughly equal to half its baryon number N_b . That, and the density of the ambient photons, which for a distance $r = \gamma \delta ct / (1 + z) > R$ decreases like $n_g(r) \approx n_g(0) (R/r)^2 \propto t^{-2}$, produce the temporal decline like t^{-2} .

The ICS of glory photons with energy ϵ by the CB electrons boosts their energies to observed energies, which satisfy $E = \gamma \delta (1 + \beta \cos \theta) \epsilon / (1 + z)$. The unknown geometry of PWNs of n*n* binaries can be very complex and different in different SHBs. The glory, however, may attain a more universal shape, in particular outside the PWNs. To illustrate the effect of the increasing anisotropy of the glory photons when a CB moves away from its launch point, consider for simplicity a CB launched along the axis of a torus-like PWN, as illustrated in Figure 4.

At the center of the PWN where $r=0$, the glory photons incident on the CB at an angle $\pi/2$ relative to its direction of motion. At a distance $r > 0$ from the center of the PWN, the glory photons intercept the CB at angles that satisfy $\cos \theta = -r / \sqrt{r^2 + R^2}$, which yields the t -dependence

$$E_p(t) = E_p(0) [1 - t / \sqrt{t^2 + \tau^2}] \quad (4)$$

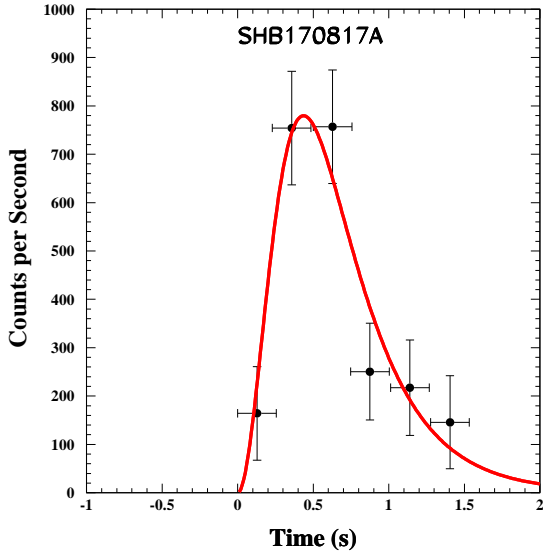


Figure 5. Comparison of the pulse shape for $E_m = 50$ keV of the first pulse of SHB170817A measured by Goldstein et al. (2017) and the CB model pulse shape as given by Eq.(6).

with $\tau = R(1+z)/\gamma\delta c$. Hence, ICS of a glory with a CPL spectrum by a highly relativistic CB yields

$$E \frac{d^2 N_\gamma}{dt dE} \propto \frac{t^2}{(t^2 + \Delta^2)^2} E^{1-\alpha} \exp(-E/E_p(0)[1-t/\sqrt{t^2 + \tau^2}]) \quad (5)$$

and $E_p \approx E_p(t = \Delta)$. For α not very different from 1, integration of $d^2 N(E, t)/dE dt$ from $E = E_m$ upwards yields,

$$N(t, E > E_m) \propto \frac{t^2}{(t^2 + \Delta^2)^2} \exp(-E_m/E_p(t)) \quad (6)$$

where $E_p(t)$ is given by Eq.(4). A best fit of Eq.(6) to the observed pulse shape (Goldstein et al. 2017) for $E_m = 50$ keV, which is shown in Figure 5, returns $\Delta = 0.54$ s $\tau = 0.65$ s, and $E_p(0) = 260$ keV. The best fit value of Δ yields $E_p \approx E_p(\Delta) = 94$ keV, while $\tau = 0.65$ s yields $R \approx 1.6 \times 10^{15}$ cm.

4. NO EXTENDED EMISSION

A considerable fraction of SHBs show an extended emission (EE) after the prompt SHB (Villasenor et al. 2005; Norris & Bonnell 2006; Fong & E. Berger 2013; Berger 2014 for a review). Such SHBs may take place in rich star clusters or globular clusters (GCs) (Dado, Dar & De Rújula 2009b), where the ratio of binary neutron stars to ordinary stars is much higher than in the regular interstellar medium of galaxies. ICS of ambient light in GCs by the highly relativistic jets, which produce the SHBs, can explain the origin of their extended

emission (Dado, Dar & De Rújula 2009b; Dado & Dar 2017). SHB170817A did not take place in a GC or a bright location in its host galaxy NGC4993 (Levan et al. 2017) and, indeed, as expected, no extended emission following its prompt emission was observed.

5. THE FIREBALL AFTERGLOW

In this chapter we show that the observed UVOIR afterglow of SHB170817A in the first two weeks after burst can be well explained by the expansion of an Arnett-type fireball (Arnett 1982) powered by several sources such as neutrino-anti neutrino annihilation outside the merging n^* s (Goodman, Dar & nussinov 1987), decay of radioactive elements within merger ejecta (Mactonova, Li & Paczynski 1998) and by the radiation, high energy particles and relativistic winds emitted from the binary n^*n^* before the merger and the nascent n^* after the merger.

It has been shown that the bolometric light curves of ordinary (Dado & Dar 2013) and superluminous (Dado & Dar 2015) SNe of Type Ia can be successfully described by a “master formula” derived from Arnett-type models. The underlying physics is complex, but the fitted values of the physical parameters turn out to be, in the cases that were studied, very close to the values expected and determined by simple physics considerations. To make this note self-contained we give in this section a brief description of the derivation of the master formula, based on energy conservation in the rest frame of a fireball powered by such energy source and losing energy by expansion and radiation.

Let t be the time after the beginning of the formation of a fireball. As long as it is highly opaque to optical photons and γ rays, its thermal energy density is dominated by black body radiation, $u(T) \approx 7.56 \times 10^{-15} T^4$ erg cm $^{-3}$ K $^{-4}$, at a temperature T that we assume for simplicity to be spatially uniform. The fireball’s total radiation energy is $U = V u$, with V the fireball’s volume. For a constant velocity of expansion, $dV/dt = 3V/t$ and the resulting energy loss is simply U/t , since $dU/dt = -p dV/dt$ and $p = u/3$ for black-body radiation.

Photon emission constitutes a second mechanism of energy loss by a fireball, corresponding to a bolometric luminosity $L \approx U/t_d$, where the photon’s mean diffusion time is $t_d \approx R^2/(c\lambda)$. The photon’s mean free path, λ , is dominated by their Thomson scattering on free electrons and positrons, $\lambda = 1/(n_e \sigma_T)$, with $n_e \propto 1/R^3$ their number density. For a fireball expanding at a constant velocity, $R = vt$, whose total number of free electrons and positrons is N_e , $t_d = t_r^2/t$, with $t_r^2 = 3N_e \sigma_T / 8\pi c v$. For a Type Ia SN, t_r can be estimated to be ~ 11 days (Dado & Dar 2015).

Neutrino-antineutrino annihilation (Goodman, Dar & Nussinov 1987), the decay of radioactive isotopes synthesized in the merger ejecta, (Lattimer & Schramm 1974), magnetic dipole radiation, relativistic winds, and high energy particles emission from the n*s contribute to the energy balance within a fireball, at a rate \dot{E} . Gathering all three contributions to \dot{U} , the time variation of U , we conclude that energy conservation implies :

$$\dot{U} \approx \dot{E} - U \left[\frac{1}{t} + \frac{t}{t_r^2} \right] \quad (7)$$

during the photospheric phase.

The solution of Eq. (7) is

$$U = \frac{e^{-t^2/(2t_r^2)}}{t} \int_0^t \bar{t} e^{\bar{t}^2/(2t_r^2)} \dot{E}(\bar{t}) d\bar{t}. \quad (8)$$

Consequently, the bolometric luminosity, $L_b = tU/t_r^2$, is given by the simple analytic expression

$$L_b = \frac{e^{-t^2/(2t_r^2)}}{t_r^2} \int_0^t \bar{t} e^{\bar{t}^2/(2t_r^2)} \dot{E}(\bar{t}) d\bar{t}. \quad (9)$$

This simple master formula, which was first derived by Dado & Dar (2013), provides an excellent description of the bolometric light curve of Supernovae Type Ia and of superluminous supernovae (Dado & Dar 2015). For a short energy deposition time $t_d \ll t_r$ by neutrino annihilation and r-processes, the late-time ($t > t_d$) behavior of Eq.(9) is

$$L_b \approx L(t_d) e^{-t^2/(2t_r^2)}. \quad (10)$$

Such a bolometric light-curve is expected if the compact remnant of the NSM170817 is a stellar black hole. A best fit of Eq.(10) to the bolometric light curve of SHB170817A reported by Smartt et al. (2017), Evans et al. (2017) and Pian et al. (2017), shown in Figure 6, yields a rather unsatisfactory $\chi^2/\text{dof} = 3.85$ for $t_r = 3.94$ d and $L(t_d) = 3.96 \times 10^{41}$ erg/s.

For a fireball that at late time ($t > t_d$) is mainly powered by a pulsar with a period P (Dar & Dado 2017 and references therein)

$$\dot{E}_{msp}(t) = L_{msp}(0)/(1+t/t_b)^2, \quad (11)$$

where $t_b = P(0)/2\dot{P}(0)$. The time dependence of \dot{E}_{msp} is slow relative to that of the rest of the integrand in Eq.(9). As a consequence it is a good approximation to factor it out of the integral, to obtain:

$$L_b \approx L_{msp}(0)[1 - e^{-t^2/2t_r^2}]/(1+t/t_b)^2. \quad (12)$$

A best fit of Eq.(12) to the bolometric light curve of SHB170817A reported by Drout et al. (2017),

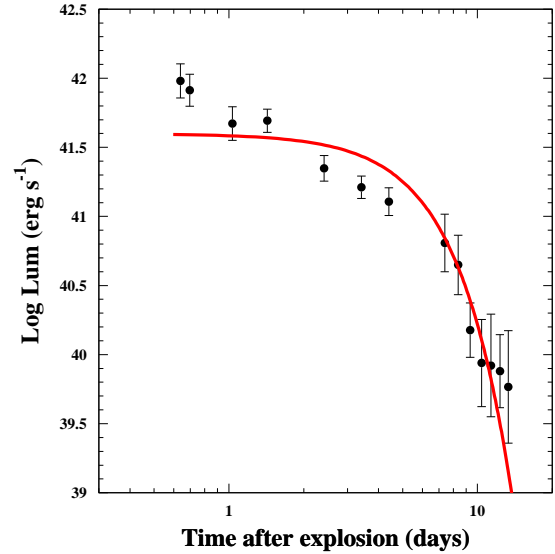


Figure 6. The best fit CB model bolometric light curve of SHB170817A to that reported by Smartt et al. (2017), Evans et al. (2017), and Pian et al. (2017), assuming the compact remnant was a black hole.

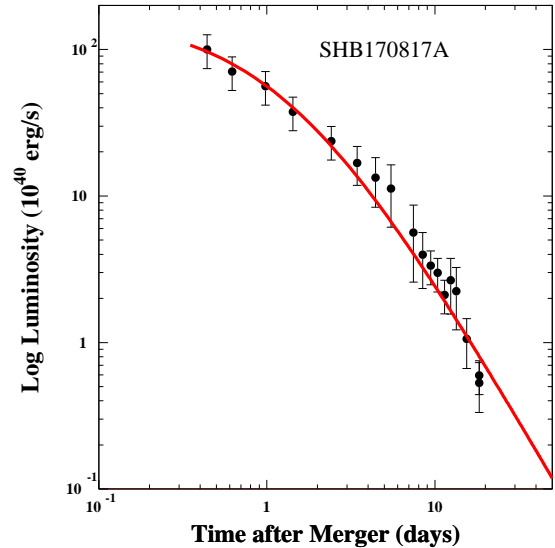


Figure 7. The best fit CB model bolometric lightcurve of SHB170817A to that reported by Drout et al. (2017), assuming a neutron star remnant.

shown in Figure 7, yields $L_{msp}(0) = 2.27 \times 10^{42}$ erg/s, $t_b = 1.15$ d, and $t_r = 0.23$ d, with an entirely satisfactory $\chi^2/\text{dof} = 1.04$. For these parameters, the approximation of Eq.(12) differs from the “exact” result of substituting Eq.(11) into Eq.(9) by 15% at the peak luminosity and $< 2\%$ at $t > 2$ d.

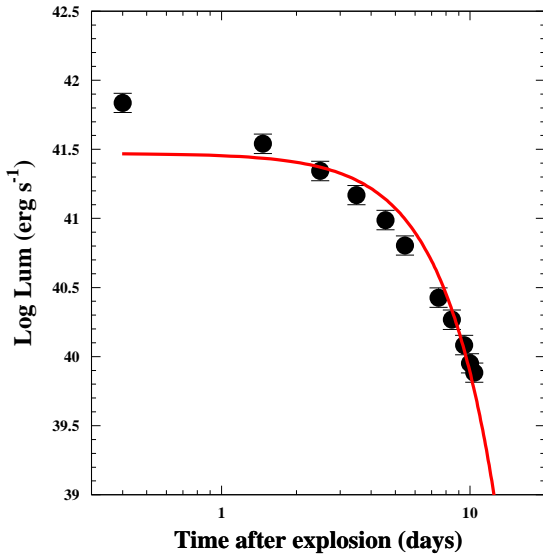


Figure 8. The best fit CB model bolometric lightcurve of SHB170817A to that reported in Cowperthwaite et al. (2017), assuming a black hole remnant.

The CB model best fits to the measured bolometric light curves of the UVOIR afterglow of SHB170817A, as shown in Figures 6,7 suggest that the compact remnant of NSM170817 is probably a pulsar rather than a stellar mass black hole.

On the other hand, best fits to the bolometric light curve reported by Cowperthwaite et al. (2017) and shown in Figures 8,9 are much less conclusive: $\chi^2/\text{dof}=1.26$ for $t_r=3.70$ d and $L(t_d)=2.95 \times 10^{41}$ erg/s for a black hole remnant, while for a neutron star remnant, $\chi^2/\text{dof}=1.0$ for $L_{msp}(0)=2.21 \times 10^{47}$ erg/s, $t_b=1.00$ d, and $t_r \ll 1$ d.

6. THE FAR OFF-AXIS AFTERGLOW

The circumburst medium in the path of a CB moving with a Lorentz factor $\gamma \gg 1$ is completely ionized by the CB's radiation. The ions of the medium that the CB sweeps in generate within it turbulent magnetic fields. The electrons that enter the CB with a Lorentz factor $\gamma(t)$ in its rest frame are Fermi accelerated there, and cool by emission of synchrotron radiation, an isotropic afterglow in the CB's rest frame. As for the rest of the CB's radiations, the emitted photons are beamed into a narrow cone along the CB's direction of motion, their arrival times are aberrated, and their energies boosted by the Doppler factor $\delta(t)$ and redshifted by the cosmic expansion.

The observed spectral energy density of the *unabsorbed* synchrotron afterglow has the form (e.g., Eq. (28)

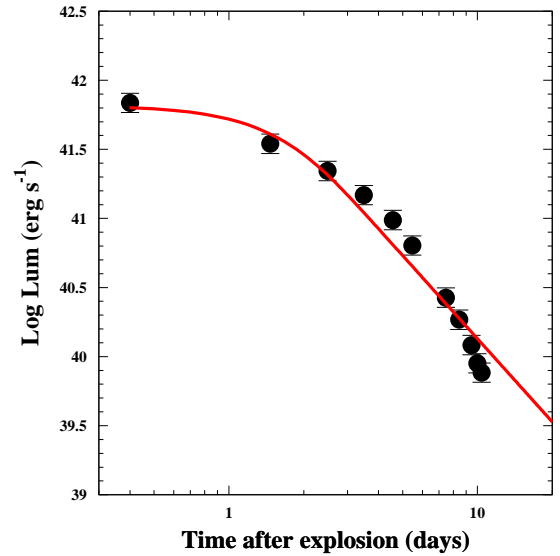


Figure 9. The best fit CB model bolometric lightcurve of SHB170817A to that reported in Cowperthwaite et al. (2017), assuming a neutron star remnant.

in Dado, Dar & De Rújula 2009a)

$$F_\nu \propto [\gamma(t)]^{3\beta-1} [\delta(t)]^{\beta+3} \nu^{-\beta}, \quad (13)$$

where β is the spectral index of the emitted radiation at a frequency ν .

The swept-in ionized material decelerates the CB's motion. Energy-momentum conservation for such a plastic collision between a CB of baryon number N_B , radius R_{CB} , and an initial Lorentz factor $\gamma_0 \gg 1$ yields the deceleration law (e.g. Eq. (3) in Dado and Dar 2012)

$$\gamma(t) = \frac{\gamma_0}{[\sqrt{(1+\theta^2 \gamma_0^2)^2 + t/t_s - \theta^2 \gamma_0^2}]^{1/2}}, \quad (14)$$

where $t_s = (1+z) N_B / (8cn\pi R_{CB}^2 \gamma_0^3)$ is the slow-down time scale. The frequency and time dependence of the afterglow implied by Eqs. (13),(14) depend only on three parameters: the product $\gamma_0 \theta$, the spectral index β , and the slow-down time-scale t_s . For $t \gg t_b$ Eq. (14) yields $\gamma(t) \propto t^{-1/4}$. and consequently a power-law decline, $F_\nu(t) \propto t^{-(\beta+1/2)} \nu^{-\beta}$. independent of the values of t_b and $\gamma(0) \theta$. For far off-axis GRBs and SHBs, as long as $\gamma^2 \theta^2 \gg 1$, $F_\nu(t)$ for $t < t_b$, rises like

$$F_\nu(t) \propto t^{1-\beta/2} \nu^{-\beta}. \quad (15)$$

In Figure 10 we compare the 6 GHz light curve of the radio afterglow of SHB170817A first discovered by Halpin et al. (2017) and followed up with the Karl G. Jansky Very Large Array (VLA), the Australia Telescope Compact Array (ATCA) and the upgraded Giant

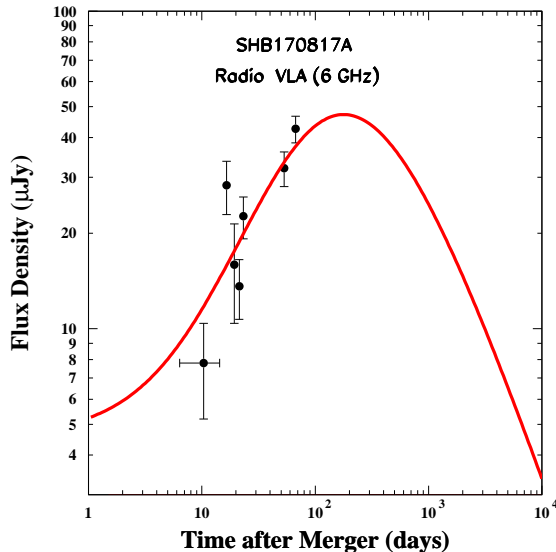


Figure 10. Comparison between the 6 GHz light curve of the afterglow of SHB170817A measured with the VLA (Hallinan et al. 2017, Mooley et al. 2018) and the light curve expected in the CB model as described in the text.

Metrewave Radio Telescope (uGMRT) and summarized by Mooley et al.(2018), and the CB model prediction. The CB model light curve was obtained from Eq.(13) with the measured radio spectral index $\beta = 0.57 \pm 0.09$ and Eq. (14) for $\gamma(t)$ where the value $\gamma(0)\theta = 5$ was obtained from the measured value $E_p = 82$ keV and the deceleration time scale $t_s = 0.167$ days from a best fit to the data.

In Figure 11 we compare the X-ray light curve measured with the Chandra X-ray observatory (CXO) and that predicted by Eqs.(13), and (14) using the same parameters as in Figure 10. Either Eq.(13) with Eq.(14), or Eq.(15) describe well the rising phase of the 0.3–10 keV X-ray light curve measured with CXO (Troja et al. 2017a,b; Margutti et al. 2017a,b; Haggard et al. 2017). The best fit value $t_s = 0.167$ d yield the product $n_b R_{CB}^2 = 2.3 \times 10^{22}/\text{cm}$, but not the individual values of the baryon density n_b of the circumburst interstellar density and of R_{CB} , the radius of the CB.

Further optical and FIR observations of the counterpart of GW170817 with the Hubble Space Telescope, which took place on 6 Dec 2017 (Levan et al. 2017) recovered the source in optical filters, but did not detect it in the infrared, where the background from the galaxy is higher. The measured magnitudes of the source in the optical bands are broadly consistent with the extrapolation from the 93 day radio epoch (Mooley et al. 2018) to the near contemporaneous observations with CXO

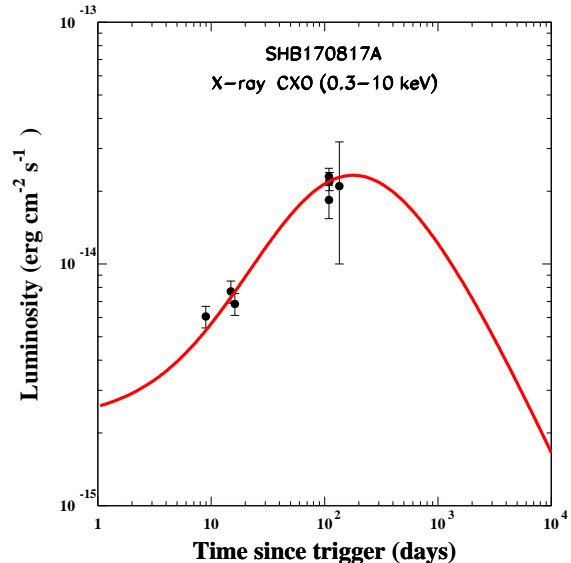


Figure 11. Comparison between the light curve of the X-ray afterglow of SHB170817A measured with the CXO (Troja et al. 2017a,b; Margutti et al. 2017a,b; Haggard et al. 2017) and the light curve expected in the CB model as described in the text.

(Troja et al. 2017a,b; Margutti et al. 2017a,b; Haggard et al. 2017).

7. SUPERLUMINAL MOTION

A very specific prediction of the CB model concerns the apparently superluminal motion in the plane of the sky, relative to the engine that produced them (Dar & De Rújula 2000b,; Dado, Dar & De Rújula 2016 and references therein), of the CBs moving towards the observer at a small but not vanishing angle θ . The apparent sky velocity of a CB relative to its emission point is given by

$$V_{\text{app}} \approx [2\gamma(t)^2 \theta / (1 + \theta^2 \gamma(t)^2)] c \quad (16)$$

with $\gamma(t)$ as in Eq.(14). For $\gamma(0)\theta \approx 5$ as estimated in Section 2 and $t_s = 0.167$ days as estimated in Section 6, $V_{\text{app}} \sim 2c/\theta \approx 400c$ for $t \ll 120$ d, and $V_{\text{app}} \approx 60c(t/10^3 \text{ d})^{-1/2}$ for $t \gg 120$ d. The estimated superluminal speed of the CB as function of time as given by Eq(16) is shown in Figure 12.

The angular displacement $\alpha(t)$ from the location of the neutron star merger to the CB's later position is:

$$\alpha(t) = c \int_0^t dt' V_{\text{app}}(t') / D_A, \quad (17)$$

with $D_A = 39.6$ Mpc the angular distance to SHB170817A in the standard cosmology.

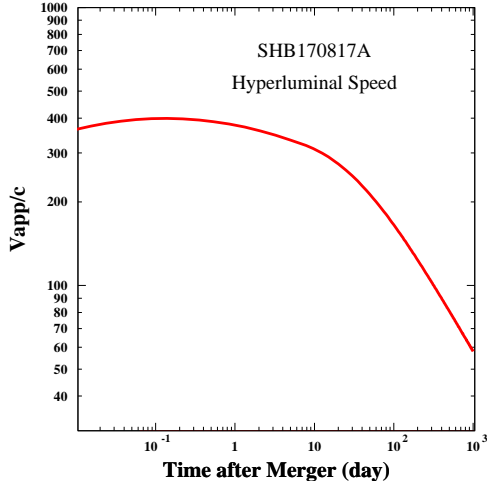


Figure 12. The estimated superluminal speed of the CB relative to the location of SHB170817A as a function of time after burst.

In a VLA or VLBI observation of SHB170817A, the angular Fresnel scale $\sqrt{\lambda/(2\pi D_A)}$ is of order $0.1 \mu\text{as}$, considerably smaller than the angular size of a CB. This may lead one to expect that a CB’s image would scintillate (Taylor et al. 2004). But typical integration times of these observations are 100 minutes. At an early time of observation ($t \sim 0$), the image of the CB of SHB170817A would move by an angle $117 \mu\text{as}$, and $48 \mu\text{as}$ at day $t = 300$. This shifting position while the data are accumulated would obliterate the scintillations (Dado et al. 2016).

8. CONCLUSIONS

The temporal and spatial coincidence of NSM170817 and SHB170817A has shown that at least a fraction, if not most SHBs, are produced in NSMs.

SHB170817A and its afterglow at redshift $z = 0.00936$ ($D_L \approx 40$ Mpc) appeared to be very different from all other SHBs with known redshift, including SHB130603B at redshift $z = 0.3564$ ($D_L \approx 2000$ Mpc), where a faint infrared emission was claimed to be the first observational evidence for a macronova produced by a NSM (e.g., Berger et al. 2013, Tanvir et al. 2013). But the observations of the low luminosity SHB170817A and its afterglow produced by NSM170817 can be naturally explained, as we have shown, by the cannonball model of GRBs, if SHB170817A was beamed along a direction far off from its line of sight and took place in the low density and low luminosity of its host galaxy NGC 4993, rather than in a dense stellar region. The CB model analysis of SHB170817A implies that like SN1998bw-

GRB980425, GW170817-SHB170817A probably was a very rare event.

In fact, based on the cannonball model of SHBs, we predicted (Dado & Dar 2017) before GW170817 that Ligo-Virgo detections of NSMs will be followed if at all, only by low-luminosity (far off-axis) SHBs, or by orphan SHB afterglows but not by ordinary SHBs. This is due to the much smaller detection horizon of Ligo-Virgo compared to the mean distance of SHBs estimated from SHBs with known redshift.

Our detailed analysis indicates that the compact remnant of NSM170817 probably was a neutron star and not a black hole, in agreement with the evidence from the afterglow of all other SHBs with known redshift and well sampled X-ray afterglow (Dado & Dar 2017).

The existence of a glory with a radius $\sim 10^{15}$ cm around the merger time is required by the CB model analysis of SHB170817A. Its origin is not clear. The most likely explanation is a PWN surrounding the binary neutron stars and powered by the emission of radiation and high energy particles and winds by one or both of them LONG before the merger. A fast expanding macronova powered by the radioactive decay of r-processed elements which exists already a day before the NSM when the merging neutron stars were separated by more than 100 times when they collided does not seem plausible. Observations of more NSM-SHB events and theoretical studies will be required in order to identify the origin of the UVOIR fireball.

We have shown that, in spite of the CB-model’s simplicity -the description of the γ -ray pulse by ICS and of the late afterglow by synchrotron radiation from a superluminally moving CB- the underlying model intrinsic and environmental parameters we extracted from both the pulse and the afterglow are very consistent. Moreover, they are compatible with our previous work on GRB and SHB pulses and afterglows.

The large superluminal speed and angular displacement that we have discussed could perhaps be observed by the VLA and VLBI follow-up measurements of the late-time location of the radio afterglow of the jet, relative to the location of SHB170817A. Such observations would be most decisive if a non-vanishing angular displacement could be measured at least two different times. It goes without saying that the precise values of the predicted displacement are quite uncertain, the crucial point being the trend shown in Figure 12.

Acknowledgments: We are particularly grateful to a referee who pointed out that, to be more complete, we ought to extract the parameters describing the cannonball and its surroundings.

ADR acknowledges that this project has received fund-

ing/support from the European Union Horizon 2020

research and innovation programme under the Marie Skłodowska-Curie grant agreement No 690575.

REFERENCES

- Abbott, B. P., et al. [Ligo-Virgo Collaboration], 2017a, PRL, 119, 161101 [arXiv:1710.05832]
- Abbott, B. P., et al. [Ligo, Virgo, Fermi, Integral Collaborations], 2017b, ApJ, 848, L12 [arXiv:1710.05834]
- Abbott, B. P. et al. [Ligo-Virgo Collaboration], 2017c, ApJ, 851, L16 [arXiv:1710.09320]
- Arnett, W. D., 1982, ApJ, 253, 785A
- Berger, E., 2014 ARA&A, 52, 43 [arXiv:1311.2603]
- Berger, E., Fong, W., Chornock, R. 2013, ApJ, 774, L23 [arXiv:1306.3960]
- Bhattacharya, D. & van den Heuvel, E. P. J., 1991, PhR, 203, 1124.
- Chamel, N. & P. Haensel, P., 2008, Living Rev. Rel. 11, 10 [arXiv:0812.3955]
- Cowperthwaite, P. S., Berger, E. Villar, V. A., et al. 2017, ApJ, 848, 17 [arXiv:1710.05840]
- Dado, S. & Dar, A., 2012, ApJ, 761, 148 [arXiv:1203.1228]
- Dado, S. & Dar, A., [arXiv:1301.3333]
- Dado, S. & Dar, A., 2015, ApJ, 809, 32 [arXiv:1301.3333]
- Dado, S. & Dar, A., 2017, arXiv:1708.04603
- Dado, S., Dar, A., De Rújula, A., 2002, A&A, 388, 1079 [arXiv:astro-ph/0107367]
- Dado, S., Dar, A., De Rújula, A., 2009a, ApJ, 696, 994 [arXiv:0809.4776]
- Dado, S., Dar, A., De Rújula, A., 2009b, ApJ, 693, 311 [arXiv:0807.1962]
- Dado, S., Dar, A., De Rújula, A., 2016, arXiv:1610.01985
- Dar, A. & De Rújula, A., 2000a, [arXiv:astro-ph/0008474]
- Dar, A. & De Rújula, A., 2000b, [arXiv:astro-ph/0012227]
- Dar, A. & De Rújula, A., 2004, PhR, 405, 203 [arXiv:astro-ph/0308248]
- Dar, A., Kozlovsky, Ben Z., Nussinov, S., Ramaty, R., 1992, ApJ, 388, 164
- Della Valle, M., AApTr, 2016, 29, Issue 2, 9
- Drout, M. R., Piro, A. L., Shappee, O.B. J. et al. 2017, Science, 358, 1570 [arXiv:1710.054431]
- Evans, P. A., Cenko, S. B., Kennea, J. K., et al. 2017, Science, 358, 1565 [arXiv:1710.05437]
- Fong, W. & Berger, E., 2013, ApJ, 776, 18 [arXiv:1307.0819]
- Gaensler, B. & Slane, P. O., 2006, ARAA, 44, 17
- Galama, T. J., Vreeswijk, P. M., van Paradijs, J., et al. 1998, Nature 395, 670 [arXiv:astro-ph/9806175]
- Goldstein, A. Veres, P., Burns, E., et al. 2017, ApJ, 848, L14 [arXiv:1710.05446]
- Goodman, J., 1986, ApJ, 308, L47
- Goodman, J., Dar, A., Nussinov, S. 1987, ApJ, 314, L7 (1987)
- Haggard, D., John J., Ruan, J. J., et al. 2017, GCN 22206
- Hallinan, G., Corsi, A., Mooley, K. P., et al. 2017, Science, 358, 1559 [arXiv:1710.05435]
- Hjorth, J., et al. 2003, Nature, 423, 847 [arXiv:astro-ph/0306347]
- Klebesadel, R. W., Strong, I. B. & Olson R. A., 1973, ApJ, 182, L85
- Kouveliotou, C., et al. 1993, ApJ, 413, L101
- Levan, A. J., Lyman, J. D., Tanvir, N. R., et al. 2017, ApJ, 848, L28 [arXiv:1710.05444]
- Lattimer, J. M., & Schramm, D. N. 1974, ApJ, 192, L145
- Li, L. X., & Paczynski, B., 1998, ApJ, 507, L59 [arXiv:astro-ph/9807272]
- Lorimer, D. R., 2008 Living Rev. Relativity, 11, 8 [arXiv:0811.0762]
- Macias-Perez, J. F., Mayet, F., Aumont, J., Dert, F. X., 2010, ApJ, 711, 417 [arXiv:0802.0412]
- Margutti, R., Berger, E., Fong, W., et al. 2017a, ApJ, 848, L20 [arXiv:1710.05431]
- Margutti, R., Fong, W., Eftekhari, T., et al. 2017b, GCN 22203
- Meegan, C. A., Fishman, G. J., Wilson, R. B., et al. 1992, Nature, 355, 143
- Meszáros, P. & Rees, M. J., 1992, MNRAS, 257, 29
- Mooley, K. P., Nakar, E., Hotokezaka, K., et al. 2018, Nature, 554, 207 [arXiv:1711.11573]
- Nicholl, M., Berger, E., Kasen, D. et al. 2017, ApJ, 848, 18 [arXiv:1710.05456]
- Norris, J. P. & Bonnell, J. T., 2006, ApJ, 643, 266 [arXiv:astro-ph/0601190]
- Norris, J. P., Cline, T. L., Desai, U. D., Teegarden, B. J., 1984, Nature, 308, 434
- Pian, E., D’Avanzo, P. S. Benetti, S. et al. 2017, Nature, 551, 67 [arXiv:1710.05858]
- Pozanenko, A. S., Barkov, M. V., Minaev, P. Yu., et al. 2018, ApJ, 852, 30 [arXiv:1710.05448]
- Shviv, N. & Dar, A., 1995, ApJ, 447, 863 [arXiv:astro-ph/9407039]
- Smartt, S.J., Chen, T. W., Jerkstrand, A., et al. 2017, Nature, 551, 75 [arXiv:1710.05841]
- Stanek, K. Z., et al. 2003, ApJ, 591, L17 [arXiv:astro-ph/0304173]
- Tanaka, S. J., & Takahara, F., 2010, ApJ, 715, 1248 [arXiv:1001.2360]
- Tanvir, N. R., Levan, A. J., Fruchter, A. S., et al. 2013, Nature, 500, 547 [arXiv:1306.4971]
- Taylor, G. B., Frail, D. A., Berger, E., Kulkarni, S.R., 2004, ApJ, 609, L1 [arXiv:astro-ph/0405300]
- Troja, E., Piro, L., van Eerten, H., et al. 2017a, Nature, 551, 71 [arXiv:1710.05433]
- Troja, E., Piro, L., van Eerten, H., et al. 2017b, GCN 22201 (2017)
- Villasenor, J. S., Lamb, D. Q., Ricker, G. R., et al. 2005, Nature, 437, 85 [arXiv:astro-ph/0510190]
- von Kienlin, A., Meegan, C., Goldstein, et al. 2017, GCN Circular 21520
- Weiler, K. W. & Panagia, N. 1978, A&A, 70, 419
- Zeh, A., Klose, S., Hartmann, D. H., 2004, ApJ, 609, 952 [arXiv:astro-ph/0311610]